Analytical and Experimental Study of Spatial Focusing by UWB Time-Reversal in Indoor Environment

T. Mavridis[1, 2]**, F. Bellens**[1, 2]**, F. Quitin**[1]**, A. Benlarbi-Delaï**[2]**, and P. De Doncker**[1]

[1]OPERA Wireless Comm. Group, Université Libre de Bruxelles, Belgium
[2]Université Pierre et Marie Curie, L2E, France

Abstract— The Time Reversal (TR) technique enables to concentrate the transmitted power on a certain area, where the receiver is located. In this paper, a closed-form analytical solution for the spatial distribution of the energy of a time-reversed system is proposed. This model is based on a plane wave expansion in a local area. Theoretical results are compared with experimental measurements to assess the validity of the Ultra-wideband TR method.

1. INTRODUCTION

The popularity of wireless communication technologies has increased the need for reliable, high-speed communications. To cope with the need for high-data rate transmissions, technologies have been proposed that use large bands of the RF spectrum, such as ultra-wideband (UWB).

Focusing techniques enable to spatially concentrate the emitted signals. It implies communications with multiple users with a higher reliability by lowering the interferences. Time Reversal (TR) appears to be an efficient technique to assess time and spatial focusing of the signal. Interesting properties of TR focusing are the high performances in a multipath environment and that the line-of-sight is not required.

The properties and the quality of the TR focusing has been widely investigated in [1, 2]. Time Reversal has already been proved in indoor [3] and intra-vehicular environments [4]. The performances have been studied in those papers but no analytical expression of the spatial distribution of the received signal has been proposed.

In this paper, a new analytic formalism based on physical properties of electromagnetic waves is developed. This formalism allows to characterize the performances of the spatial focusing of the TR method. Furthermore a study of the optimization and the tradeoffs between different wave parameters has been done. Finally, experiments are presented to assess the validity of the theoretical results.

The paper is organized as follows. In Section 2, the TR model of the spatial distribution of the energy is proposed. The analysis of the different parameters introduced in Section 2 is presented in Section 3. The measurement results and the comparison with the theory are presented in Section 4. Finally, Section 5 concludes the paper.

2. TIME REVERSAL MODELLING

2.1. Energy Calculation

The TR technique is a two-step transmission method. First, the receiver sends a pilot broadcast signal to the transmitter. The transmitter learns the channel impulse response $h(\tau)$ by sampling a received (known) signal. The second step consists of the transmission itself: the transmitter filters the signal with the time reversed version of the impulse response $h^*(-\tau)$ (where * is the complex conjugate operation). Considering that the channel remains static, the receiver will obtain the transmitted signal through the equivalent channel $h(\tau) \otimes h^*(-\tau)$ as described in [4] where $\otimes$ represents the convolution operation. In this paper, the total energy $\mathcal{E}$ over the bandwidth is considered by integrating the equivalent channel. If the transmitted signal has unit energy, the energy of the received signal will be the following:

$$\mathcal{E}(\vec{r}) = \int_0^\infty |h_{\vec{r}}(\tau) \otimes h_{\vec{r_0}}^*(-\tau)|^2 d\tau \tag{1}$$

where $\vec{r}$ is the position of the evaluated energy, and $\vec{r_0}$ is the position where the energy is being focused (the receiver position). The Parseval equality is then used in (1) to introduce the frequency response $H(f)$ which is the Fourier transform of the impulse response $h(\tau)$:

$$\mathcal{E}(\vec{r}) = \int_{\Delta f} |H_{\vec{r}}(f) H_{\vec{r_0}}^*(f)|^2 df \tag{2}$$

where Δf is the bandwidth.

2.2. Plane Wave Expansion

To resolve Equation (2), a mathematical expression of the frequency response depending on the environment parameters has to be introduced. The following plane wave expansion has been chosen:

$$H_{\vec{r}}(f) = \sum_{i=0}^{N} a_i e^{j\phi_i} e^{-j\omega\tau_i} e^{-j\vec{\beta}_i \cdot \vec{r}} \tag{3}$$

where a_i, ϕ_i and τ_i are, respectively, the amplitude, the phase and delay of the ith wave, N is the number of waves and ω is the pulsation of the signal. In this equation, $\vec{\beta}_i = \omega/c \cdot \vec{1}_i$ is the wave vector where c is the speed of light and $\vec{1}_i$ is the propagation direction of the ith wave. Those parameters are evaluated at $\vec{r}_0$ position. To develop an analytical solution of the time reversed energy, a local spatial area where those parameters can be assumed as constant is introduced.

The size of this local area is defined by studying the bandwidth availability and the phase shift $\beta\Delta R$ of a wave calculated in two extremal positions (ΔR is the distance between those positions and by consequence, it is the size of the local area). It can be shown [6] that $\beta\Delta R$ has to be smaller than $\frac{2\pi f_c}{\Delta f}$ where f_c is the carrier frequency. Finally, it infers that $\Delta R_\lambda < \frac{f_c}{\Delta f}$ where the size of the local area has been defined in wavelength unit. This condition defines the spatial size of the area where the energy distribution will be assessed in this paper.

2.3. Spatial Time Reversed Energy

To simplify (3), a change of coordinate system is done by choosing $\vec{r}_0$ as the center of the local area by defining $\vec{r}_0 = \vec{0}$, $\vec{r} = \vec{\Delta r}$,

$$H_{\vec{r}}(f) = \sum_{i=0}^{N} a_i e^{j\phi_i} e^{-j\omega\tau_i} e^{-j\vec{\beta}_i \cdot \Delta\vec{r}} \quad \text{and} \quad H_{\vec{r}_0}(f) = \sum_{i=0}^{N} a_i e^{j\phi_i} e^{-j\omega\tau_i} \tag{4}$$

The vector $\Delta\vec{r}$ is introduced as the difference between the position where the energy is calculated $\vec{r}$ and the focus position $\vec{r}_0$. By introducing (4) in (2) and by integrating over the band $[f_c - \Delta f/2, f_c + \Delta f/2]$, a closed-form expression is obtained for the spatial distribution of the energy:

$$\begin{aligned}
\mathcal{E}(\vec{r}) = \sum_{i=1}^{N}\sum_{h=1}^{N}\sum_{l=1}^{N}\sum_{m=1}^{N} \alpha_{ihlm} \bigg(&\cos\left(\Phi_1^{ihlm} + 2\Psi_1^{ihlm} f_c\right)\operatorname{sinc}\left(\Psi_1^{ihlm}\Delta f\right) \\
&+ \cos\left(\Phi_2^{ihlm} + 2\Psi_2^{ihlm} f_c\right)\operatorname{sinc}\left(\Psi_2^{ihlm}\Delta f\right)\bigg)
\end{aligned} \tag{5}$$

where the following simplifications of notations have been done:

$$\begin{aligned}
\alpha_{ihlm} &= a_i a_h a_l a_m \\
\Phi_1^{ihlm} &= \phi_i - \phi_h - \phi_l + \phi_m \\
\Phi_2^{ihlm} &= \phi_i - \phi_h + \phi_l - \phi_m \\
\Psi_1^{ihlm} &= \pi\left(\tau_i - \tau_h - \tau_l + \tau_m + \Delta\vec{1}_{lm}\frac{\Delta\vec{r}}{c}\right) \\
\Psi_2^{ihlm} &= \pi\left(\tau_i - \tau_h + \tau_l - \tau_m - \Delta\vec{1}_{lm}\frac{\Delta\vec{r}}{c}\right).
\end{aligned} \tag{6}$$

In (6), $\Delta\vec{1}_{lm}$ has been defined as the difference of propagation direction between the lth and mth wave and is equal to $\vec{1}_l - \vec{1}_m$. It can be observed in (5) that the spatial distribution of the energy depends on the number of waves N, the angle of incidence, magnitude, phase and delay of the waves but also on the carrier frequency and the bandwidth. This closed-form solution allows to define the best combination of parameters in order to improve the focusing properties of the TR technique.

3. SIMULATIONS

3.1. Conditions

A system defined by its bandwidth Δf can sample the signal each $1/\Delta f$. To be considered as different, two waves must have a difference of arrival time higher than this sampling time. If this condition is not met, the waves will be sampled in the same tap and be considered as the same one. In the following sections, it will be assumed that the difference between the delays in the simulations is always higher than $1/\Delta f$. To allow 2D focusing, it can be seen in (5) that at least three waves are needed. In the next sections, an assumption will be made that at least three waves are available. Those conditions are easily verified in indoor environments.

3.2. Delay Spread, Phases and Number of Waves

The phases and delays can not be fixed in a deterministic way because of their high dependence on the environment parameters. In this case, they will be kept random. In Figure 1, the phases are varying uniformly in $[0, 2\pi]$ and the delays are chosen uniformly in $[0, 10/c]$ to study their influence in the spatial energy distribution.

It can be seen in Figure 1, that the delay and phase have no influence on the spatial distribution of the energy. The focus radius at $-1.5\,\text{dB}$ is about $0.2\lambda_c$. An increasing number of waves does not change the focus radius but decreases the side lobes.

3.3. Angular Spread

In Figure 2(b), the focus area at a relative energy of $-1.5\,\text{dB}$ is studied. The simulation was based on the system presented in Figure 2(a). This system is made up of three plane waves incident on the focus point. The propagation direction of the plane wave 1 has been taken for reference. The angle θ_1 (θ_2) is defined by the angle between the first wave and the second (third) one. On Figure 2(b), the normalized area has been presented. It is the area where the energy is above $-1.5\,\text{dB}$ divided by the optimal case (the minimum area is obtained when $\theta_1 = \theta_2 = 120°$). This figure allows to study by how much times the focus size is growing when the angular spread is modified.

(a)   (b)
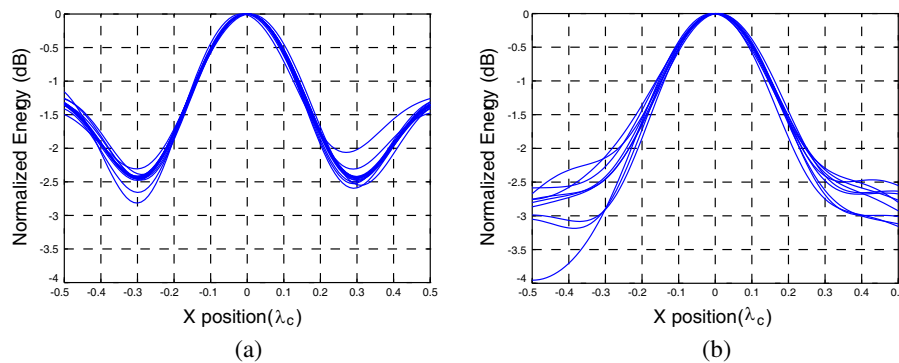
Figure 1: Spatial distribution of the energy for random phases and delays. (a) $N = 3$, (b) $N = 10$.

(a)   (b)
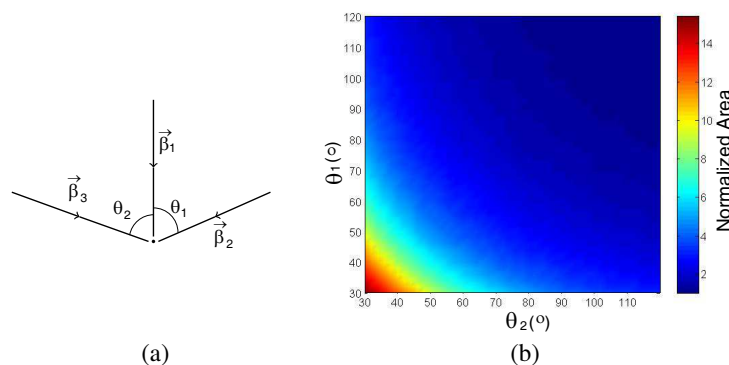
Figure 2: Focus spot normalized (by the optimal case) area. Study of the variation of the angular incidence of the secondary waves. (a) Analyzed system mad up three incident waves. (b) Normalized area of the focus point when the angular spread varies.

By taking the worst case represented in Figure 2 ($\theta_1 = \theta_2 = 30°$), it can be seen that the focus area can be fourteen times higher than the optimal case (in that case the signal can not be considered as spatially focused). It can be inferred that an optimal focus quality is obtained when the angular spread is maximized. Others simulations have been calculated for systems made up of different numbers of wave N and the best focus spot size is always obtained for an uniform angular arrival.

3.4. Carrier Frequency and Bandwidth

If a maximal angular spread is considered, the last parameters that can affect the distribution of energy are the carrier frequency and the bandwidth. In this case, it can be observed that the bandwidth has almost no effect on the focus spot size but can decrease the height of the side lobes. In fact, the increase of the bandwidth has the same effect on the energy distribution as the number of waves (see Section 3.1).

As presented in Figure 1, the focus radius is about $0.2\lambda_c$ and it can be observed that this value does not change with the carrier frequency. When this value is converted in spatial metrics (not in terms of wavelength), it can be inferred that the focus spot width is decreasing as the carrier frequency is going up. It can be shown that this relation vary according to $1/f_c$.

3.5. Conclusion about the Parameters Optimization

Each parameter has a different influence on the spatial energy distribution. The system resources (frequency parameters) can be modified and optimized but the physical parameters exclusively depend on the environment and are generally fixed. In order to design the focus spot size, the carrier frequency and the angular spread have to be increased. The last one can be modified by using a multiple antennas system. In order to increase the discrimination between the focus point energy and side lobes, the bandwidth and the number of waves have to be as high as possible. One way to increase the multipath is to obstruct the line-of-sight between the transmitter and receiver (see Section 4).

4. EXPERIMENTAL RESULTS

4.1. Measurement Setup

Experimental measurements were performed in order to assess the performances of the theoretical results of Sections 2 and 3. Three transmit antennas $(\text{Tx})_i$ were used to increase the angular spread. The line-of-sight has been obstructed to increase the multipath. The channel frequency responses $H_i(f)$ were collected with a four-port VNA in an indoor environment with $f_c = 6.85\,\text{GHz}$ and $\Delta f = 7.5\,\text{GHz}$ by a step of $7.5\,\text{MHz}$. The receiver (Rx) was moved on a $10\,\text{cm}$ square grid by a $2\,\text{mm}$ step. The Rx has been moved with an automatic positioning device. The TR is applied as a posteriori treatment thanks to Equation (2).

In order to simulate a SISO (single input single output) with a high angular spread, the transfer function of the system will be defined as $H_{\text{system}}(f) = H_1(f) + H_2(f) + H_3(f)$ where the $H_i(f)$'s are the transfer functions of the channel between the receiver (Rx) and ith transmitter (Txi).

4.2. Measurement Results

An example of the spatial distribution of the energy by applying TR is given in Figure 3. It can be seen that the focal radius is about $0.2\lambda_c$. The location of the focal spot can be moved, and similar results are observed when the receiver position is changing.

As can be seen in Figure 3, the decrease of the bandwidth does not change the size of the focus area but the side lobes are higher in the (b) case than the (a) one as predicted in Section 3.4. These results can be compared with the theoretical conclusions and can assess the validity of our TR model.

4.3. Comparison with Theory

To examine the measurement results, the theoretical Equation (5) requires the determination of the parameters of the plane waves. The use of a ray identification algorithm (SAGE [5]) is required. It models the spatial distribution of the impulse response and can work out the plane waves parameters: a_i, ϕ_i, τ_i and θ_i. By using the model developed in the previous part, the experiment results can be compared with the theory.

As can been seen, the energy level and the area around the focal point fits with the theoretical simulation. Others comparisons have been done by varying the different parameters to assess the validity of this model. The results were successful.

(a)   (b)
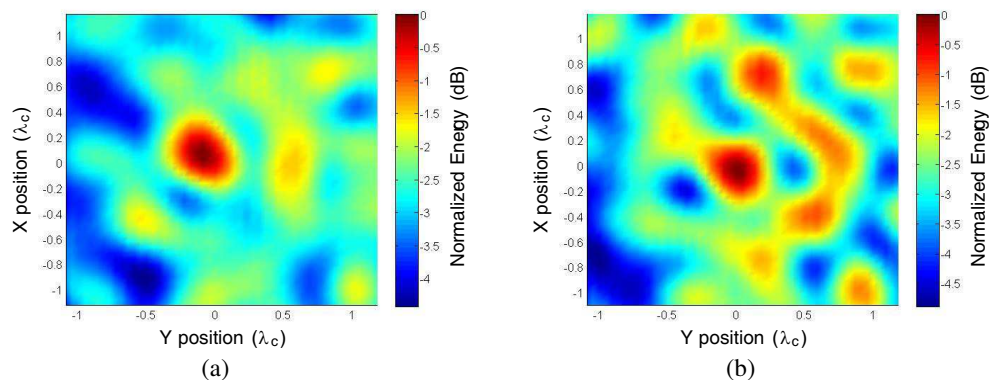
Figure 3: Relative energy received for $f_c = 6.85\,\mathrm{GHz}$. (a) $\Delta f = 7.5\,\mathrm{GHz}$, (b) $\Delta f = 1.5\,\mathrm{GHz}$.
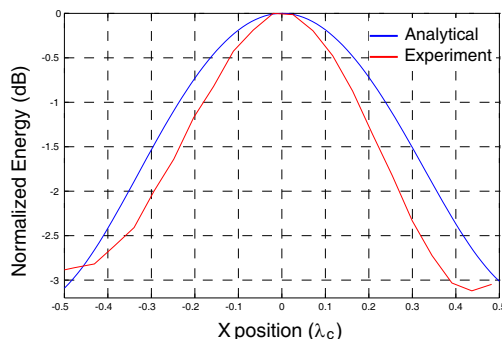
Figure 4: Relative energy received for three base stations simulating a SISO system. Comparison between the experiment result and the analytical calculations.

5. CONCLUSION

In this paper, a new analytical formalism of the Time Reversed spatial energy distribution based on a local plane wave expansion has been developed. UWB Experiments has been done to prove the validity of the energy distribution in a local area around the receiver position described by the model presented in this paper. Those analytical results show the parameters influence on the focusing quality and allow to make an optimisation of the system design. The Time Reversed focusing method has also been applied in different (indoor and intra-vehicular) environments to test this modelling and the results were successful. We have also shown that the evolution of the energy distribution follows the equations presented here when the parameters described in Section 3, are modified.

The analytical equations described here can be used to make the design of the environment and predict the focusing quality in a static channel when a UWB Time Reversal system is used.

REFERENCES

1. Oestges, C., A. Kim, G. Papanicolaou, and P. Paulraj, "Characterization of space-time focusing in time-reversed random fields," *IEEE Trans. Antennas Prop.*, Vol. 53, 283–293, Jan. 2005.
2. Emami, E., J. Hansen, A. D. Kim, G. Papanicolaou, A. Paulraj, D. Cheung, and C. Prettie, "Predicted time reversal performance in wireless communications using channel measurements," *Proc. IEEE Comlet*, 2002.
3. Zhou, C. and R. C. Qiu, "Spatial focusing of time-reversed UWB electromagnetic waves in a hallway environment," *Proc. IEEE 38th Southeastern Symp. on Syst. Theo.*, Cookeville, TN, USA, 2006.
4. Bellens, F., F. Quitin, J.-M. Dricot, F. Horlin, A. Benlarbi-Delai, and P. De Doncker, "Performance evaluation of time reversal in intra-vehicular environment," *Proc. Eur. Antennas and Propagation Conf. (EUCAP)*, 2011.
5. Quitin, F., C. Oestges, F. Bellens, S. Van Roy, F. Horlin, and P. De Doncker, "Extracting specular-diffuse clusters from MIMO channel measurements," submitted to *22nd Symposium on Personal, Indoor and Mobile Radio Communications (PIRMC)*, 2011.
6. Oestges, C. and B. Clerckx, "MIMO wireless communications," *Elsevier Academic Press*, 42–45, 2007.